Coarsening and Microsegregation during Solidification of Ni-Al-Cr Dendritic Monocrystals

J. J. MONTOYA-CRUZ, R. KADALBAL, T. Z. KATTAMIS, and A. F. GIAMEI

Dendritic monocrystals of nickel-rich Ni-Al-Cr alloys were directionally solidified at rates ranging from 0.05 to 2.00 m per hour, under gradients of 8×10^3 and 20×10^3 K per meter. It was found that if growth is cellular dendritic, the cellular dendritic spacing exhibits the same dependence on growth rate or local cooling rate as does the secondary dendrite arm spacing in columnar dendrites. A study of the isothermal coarsening kinetics of the dendritic solid indicated that an increase in chromium or aluminum concentrations slowed down coarsening, yielding finer cast microstructures. At equal atomic percental increase in concentration the effect of chromium was more significant than that of aluminum in refining the dendritic structure. With increasing local cooling rate the maximum solute concentration remained practically constant, the minimum solute concentration slightly decreased, the segregation ratio slightly increased, and the volume fraction of nonequilibrium interdendritic γ' phase increased substantially. This phase dissolved during crystal pulling faster in crystals that were grown at a higher rate. The homogenization kinetics of aluminum and chromium were established both analytically and experimentally. A longer time was necessary for chromium than for aluminum in order to achieve the same index or residual segregation.

I. INTRODUCTION

IN previous publications the unidirectional growth of dendritic monocrystals of Ni-Al-Ta alloy was used to establish: (1) the coarsening kinetics of dendrites,[1] both isothermally at a temperature between the liquidus and the eutectic temperatures, as well as during continuous solidification; (2) the distribution of solute during and after solidification and its dependence on local cooling rate;[2] (3) the effect of dendritic coarsening on this distribution;[2] (4) the solution kinetics of the nonequilibrium interdendritic γ' phase;[2] and the homogenization kinetics of aluminum and tantalum,[3] both isothermally and during crystal pulling.

An increase in tantalum or aluminum contents was found to slow down coarsening. At equal percental increase in concentration the effect of tantalum was more significant than that of aluminum. The evolution of the solute distribution profile across the dendritic structure during solidification was found to be controlled by back-diffusion in the solid rather than dendritic coarsening. With increasing local cooling rate the maximum solute concentration, C_M, remained practically unchanged, the minimum solute concentration, C_m, slightly decreased, the segregation ratio, $S = C_M/C_m$, increased, and so did the volume fraction of nonequilibrium interdendritic γ' phase. This phase dissolved during crystal pulling much faster at higher crystal growth rates. Solution kinetics were found to depend on the dimensionless parameter $D\theta/L^2$, where D is diffusivity of solute at a given temperature at which a given transverse cross section of the crystal remains for a time θ and L is half the primary dendrite arm spacing. A diffusion model was introduced to analyze homogenization kinetics. Aluminum was found to homogenize much faster than tantalum during an isothermal treatment. It also homogenizes appreciably during crystal pulling.

A similar investigation was conducted on the Ni-Al-Cr system and was ultimately extended to the quaternary Ni-Al-(Ta + Cr) system. The work on Ni-Al-Cr is reported herein.

II. EXPERIMENTAL PROCEDURE

The experimental procedure used was identical to that previously described.[1,2] Dendritic monocrystals of Ni-14.0 at. pct Al-4.2 at. pct Cr, Ni-18.0 at. pct Al-4.1 at. pct Cr, Ni-14.0 at. pct Al-8.2 at. pct Cr, Ni-19.2 at. pct Al-11.90 at. pct Cr, and Ni-14.8 at. pct Al-8.2 at. pct Cr were solidified under a thermal gradient of 8×10^3 K/m and at growth rates of 0.05, 0.10, 0.25, and 2.00 m per hour, as shown in the Table. Steady state growth of the dendritic solid was interrupted at a given moment by pneumatically pulling the crucible out of the furnace at very high speed and into a water bucket, thus quenching the remaining liquid. The monocrystals were sectioned transversely at different temperature levels at the time of quench. The temperature corresponding to each section at the moment of quench was measured as described previously,[4] and the distribution profiles of aluminum and chromium across each section were established by electron microprobe analysis. Transverse sections made below the ternary eutectic temperature were used for measuring the volume fraction of the remaining undissolved nonequilibrium γ' phase and establishing its solution kinetics during crystal pulling. For studying the isothermal solution kinetics of interdendritic γ' pulling of the monocrystals was arrested at a given moment for different lengths of time prior to quenching the remaining liquid. The remaining volume fraction of interdendritic γ' was measured in cross sections corresponding to the same temperature in the various specimens and plotted *vs* holding time. Cross sections taken within the mushy zone were used for studying the isothermal coarsening kinetics of the solid at various temperatures between the liquidus and the eutectic temperature.[1] This was done by measuring the solid-liquid

J. J. MONTOYA-CRUZ, formerly Graduate Assistant, University of Connecticut, is now with Instituto Tecnologico de Morelia, Morelia, Michoacan, Mexico. R. KADALBAL, Graduate Assistant, and T. Z. KATTAMIS, Professor, are both with the Department of Metallurgy, University of Connecticut. A. F GIAMEI is Senior Consulting Scientist with United Technologies Research Center, East Hartford, CT.

Manuscript submitted September 14, 1981.

ISSN 0360-2133/82/0711-1153$00.75/0

interface area per unit volume of solid, S_v, at various locations corresponding to these temperatures in all specimens and plotting these data *vs* isothermal coarsening time.

In order to study the dependence of dendrite arm spacing on growth rate, R, and average thermal gradient, G, in the mushy zone, two additional dendritic monocrystals of Ni-18.0 at. pct Al-4.1 at. pct Cr were pulled under a gradient of about 20×10^3 K/m and at growth rates of 0.10 and 0.25 m per hour.

For the homogenization studies specimens (1 to 1.5×10^{-3}m thick) were prepared by sectioning transversely the single crystals at distances of about 10 to 15×10^{-3}m from the dendrite tips. At these distances the interdendritic nonequilibrium γ-γ' eutectic, or the γ' phase resulting from its divorce, were completely eliminated by dissolution during crystal pulling. Specimens were encapsulated under vacuum conditions, homogenized at 1473 K or 1588 K for six and 12 hours and air cooled. Microsegregation in these specimens was investigated by electron microprobe analysis.

III. RESULTS AND DISCUSSION

In plotting dendrite arm spacings *vs* growth rate or local cooling rate difficulties may arise when growth conditions are such that the columnar dendritic microstructure is replaced by a cellular dendritic. Intuitively, but erroneously, cellular dendritic spacings are often assimilated with primary dendrite arm spacings. It will be shown below that cellular dendritic spacings should rather be reported on the secondary dendrite arm spacing curve.

The growth conditions corresponding to the morphological transition between cellular and columnar dendrites for Ni-18.0 at. pct Al-4.1 at. pct Cr alloy are shown in Figure 1. Among the five monocrystals processed, monocrystal A was grown under $G = 8 \times 10^3$ K/m and $R = 0.25$ m per hour and monocrystal B under $G = 20 \times 10^3$ K/m and at $R = 0.10$ m per hour. The corresponding local cooling rate, ε, for both monocrystals was therefore the same and equal to 0.55 K per second.

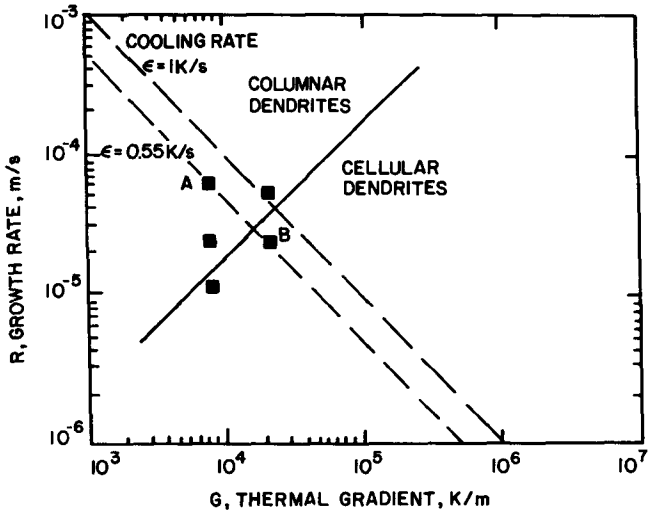

Fig. 1—G-R-ε diagram indicating morphological transition. Ni-18.0 at. pct Al-4.1 at. pct Cr alloy.

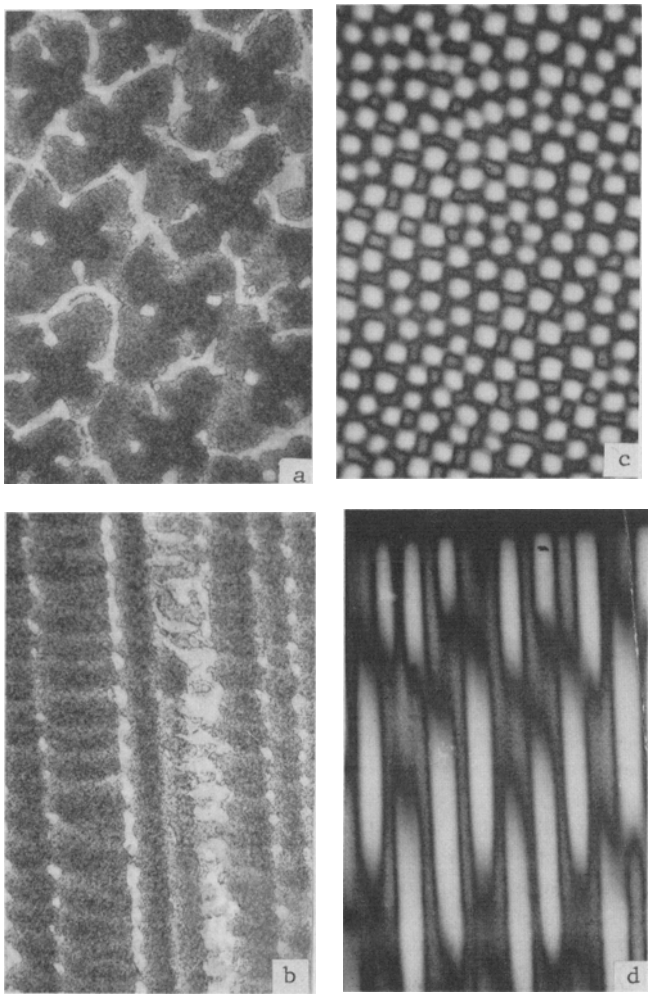

Fig. 2—Photomicrographs of sections of 2 dendritic monocrystals, A and B, of Ni-18.0 at. pct Al-4.1 at. pct Cr alloy. Magnification 40.7 times. (*a*) and (*b*) are transverse and longitudinal sections, respectively, of crystal A. $G = 8 \times 10^3$ K/m, $R = 0.25$ m/h. (*c*) and (*d*) are transverse and longitudinal sections, respectively, of crystal B. $G = 20 \times 10^3$ K/m, $R = 0.10$ m/h.

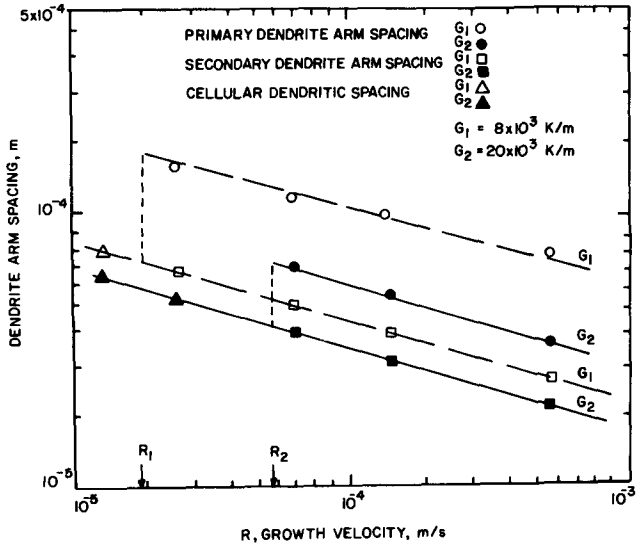

Fig. 3—Primary and secondary dendrite arm spacings, and cellular dendritic spacing *vs* growth rate for $G_1 = 8 \times 10^3$ and $G_2 = 20 \times 10^3$ K/m. Ni-18.0 at. pct Al-4.1 at. pct Cr alloy.

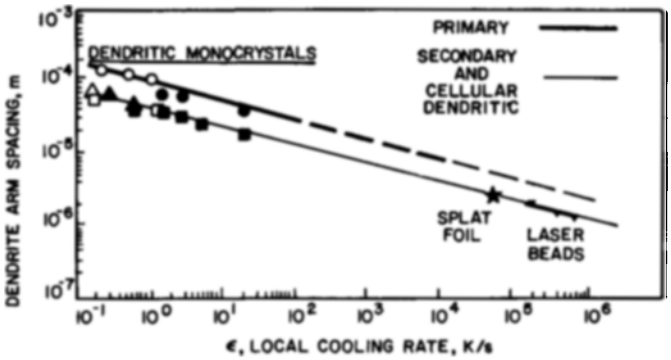

Fig. 4 — Primary, secondary, and cellular dendritic spacings *vs* local cooling rate. Ni-18 0 at. pct Al-4 1 at. pct Cr alloy.

Fig. 5 — Photomicrographs of longitudinal sections of Ni-14.0 at. pct Al-4.2 at. pct Cr dendritic monocrystals continuously grown at 0.25 m/h and coarsened for (*a*) 0 s and (*b*) 90 s prior to quenching the remaining liquid. Magnification 39.5 times.

Photomicrographs of longitudinal and transverse sections of these monocrystals are shown in Figure 2. Monocrystal A is columnar dendritic and B is cellular dendritic. The cellular dendritic spacing in monocrystal B is equal to the secondary dendrite arm spacing in monocrystal A, not to the primary. This would indicate that coarsening, which is known to control secondary dendrite arm spacing, controls also cellular dendrite spacing in cellular dendrites. Figure 3 illustrates the dependence of primary and secondary dendrite arm spacings, and of cellular dendritic spacing on growth velocity for two gradients: 8×10^3 and 20×10^3 K/m. For each gradient the cellular dendritic spacings fall on the extension of the secondary dendrite arm spacing curve. The critical growth rates R_1 and R_2 at which the transition between cellular dendritic and columnar dendritic structures occur for G_1 and G_2, respectively, are indicated in the same Figure. These values were deduced from Figure 1. The data points of Figure 3 were reported in Figure 4 *vs* local cooling rate $\varepsilon = G \cdot R$. Again secondary dendrite arm spacings and cellular dendritic spacings fall on one and the same curve, and primary dendrite arm spacings on another.

A. *Dendrite Coarsening*

Isothermal coarsening kinetics were experimentally determined for three alloy compositions: Ni-14.0 at. pct Al-4.2 at. pct Cr, Ni-18.0 at. pct Al-4.1 at. pct Cr, and Ni-14.0 at. pct Al-8.2 at. pct Cr. Figure 5 illustrates photomicrographs of longitudinal sections of Ni-14.0 at. pct Al-4.2 at. pct Cr dendritic monocrystals grown at 0.25 m per hour and coarsened for: (a) 0 seconds and (b) 90 seconds, prior to quenching the remaining liquid. The variation of Sv/Sv_0, where Sv_0 is the value of Sv for time 0 of coarsening, *vs* isothermal coarsening time is illustrated in Figure 6 for a temperature of 1676 K, between the liquidus and the ternary eutectic temperature and for the three alloy compositions. These curves indicate that: (1) at constant chromium concentration (curves A and B) an increase in aluminum concentration slows down coarsening; (2) at constant aluminum concentration (curves B and C) an increase in chromium concentration drastically slows down coarsening and; (3) at equal atomic percental increase in concentration the effect of chromium is more significant than that of aluminum. A comparison with the coarsening behavior of the Ni-Al-Ta alloy system[1] clearly shows that an increase in tantalum concentration slows down coarsening

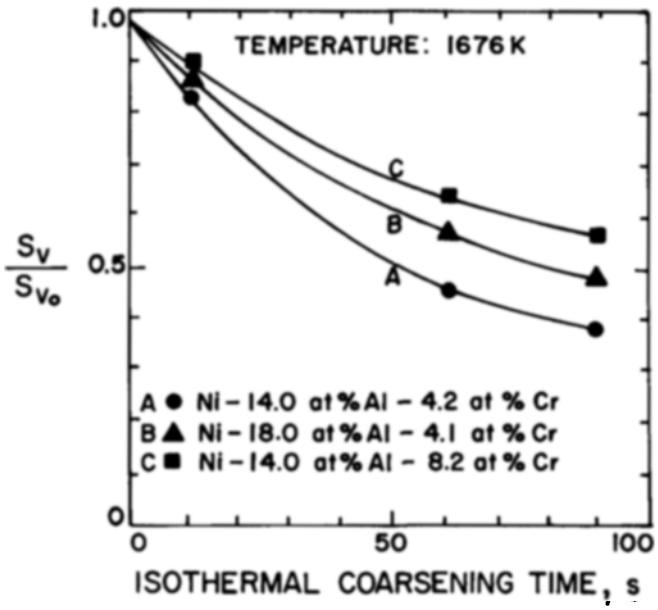

Fig. 6 — Variation of Sv/Sv_0 *vs* isothermal coarsening time at 1676 K and composition. Experimental curves.

more substantially than does an equal atomic percental increase in chromium concentration. The effect of aluminum and chromium contents on coarsening kinetics is further illustrated in Figure 7. In this figure the coarsening time required for a 50 pct reduction of Sv_0, or $Sv/Sv_0 = 0.5$, at 1676 K is plotted *vs* chromium concentration of alloys of compositions: Ni-14.0 at. pct Al-3.2 at. pct Cr, Ni-14.0 at. pct Al-4.2 at. pct Cr, Ni-14.0 at. pct Al-6.3 at. pct Cr, and Ni-14.0 at. pct Al-8.0 at. pct Cr and *vs* aluminum concentration for alloys of compositions: Ni-12.0 at. pct Al-4.2 at. pct Cr, Ni-14.0 at. pct Al-4.2 at. pct Cr, Ni-16.0 at. pct Al-4.2 at. pct Cr, and Ni-18.0 at. pct Al-4.2 at. pct Cr. Growth conditions of these dendritic monocrystals are given in the Table. Figure 7 shows very clearly that at equal percental concentration increases, chromium is more effective than aluminum in slowing down coarsening kinetics,

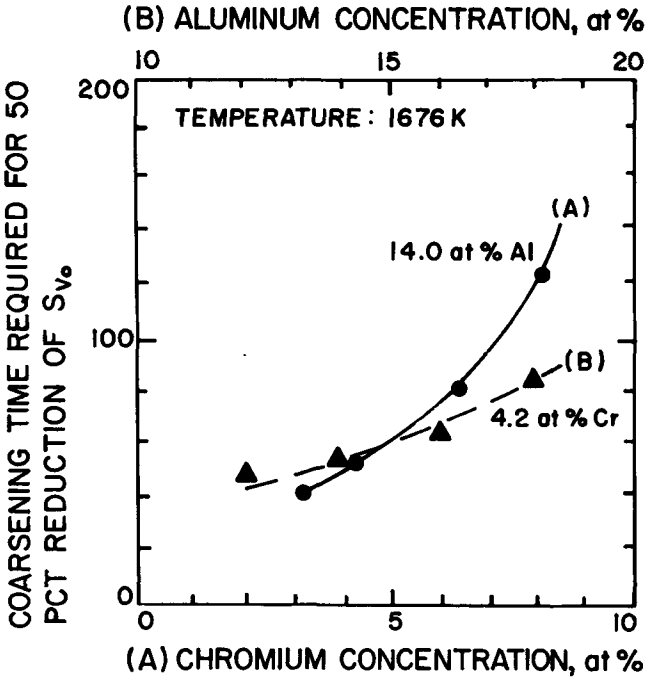

Fig. 7—Variation of the coarsening time at 1676 K required for a 50 pct reduction of Sv_0 *vs* chromium concentration at 14.0 at. pct Al and aluminum concentration at 4.2 at. pct Cr.

Table I. Composition of Dendritic Monocrystals and Growth Conditions

R = 0.05, 0.10, 0.25, and 2.00 m/h; $G = 8 \times 10^3$ K/m
Ni-14.0 at. pct Al-4.2 at. pct Cr
Ni-18.0 at. pct Al-4.1 at. pct Cr
Ni-14.0 at. pct Al-8.2 at. pct Cr
Ni-19.2 at. pct Al-11.90 at. pct Cr
Ni-14.8 at. pct Al-8.2 at. pct Cr
R = 0.10 and 0.25 m/h; $G = 20 \times 10^3$ K/m
Ni-18.0 at. pct Al-4.1 at. pct Cr
R = 0.10 m/h; $G = 8 \times 10^3$ K/m
Ni-14.0 at. pct Al-3.2 at. pct Cr
Ni-14.0 at. pct Al-6.3 at. pct Cr
Ni-14.0 at. pct Al-8.0 at. pct Cr
Ni-12.0 at. pct Al-4.2 at. pct Cr
Ni-16.0 at. pct Al-4.2 at. pct Cr
Ni-18.0 at. pct Al-4.2 at. pct Cr

yielding finer dendritic microstructures, all other solidification conditions remaining the same. The effect of temperature on the coarsening kinetics of Ni-14.0 at. pct Al-4.2 at. pct Cr is illustrated in Figure 8. These kinetics become faster with increasing temperature, as previously established[1,5] for other systems.

B. *Effect of Growth Conditions on Microsegregation*

The distribution of aluminum and chromium across the dendrites was determined at 1661 K, a temperature which, as established by DTA, is about 2 K below that of the ternary eutectic temperature at which solidification was completed.

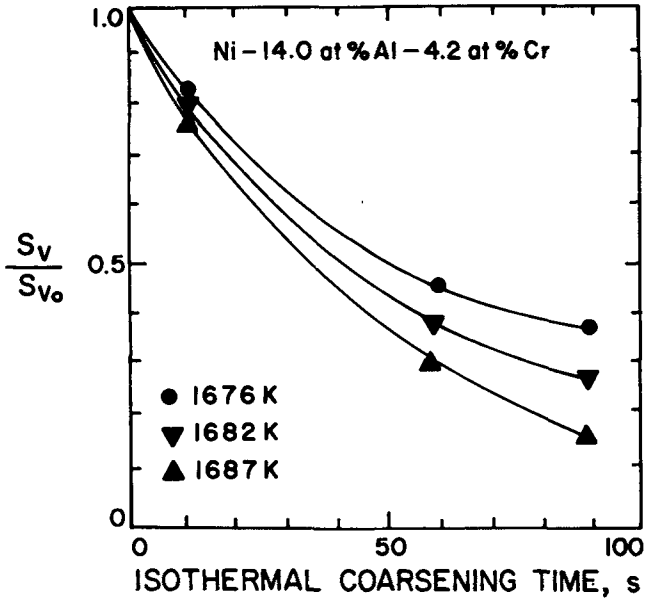

Fig. 8—Variation of Sv/Sv_0 *vs* isothermal coarsening time and temperature. Experimental curves. Ni-14.0 at. pct Al-4.2 at. pct Cr dendritic monocrystals.

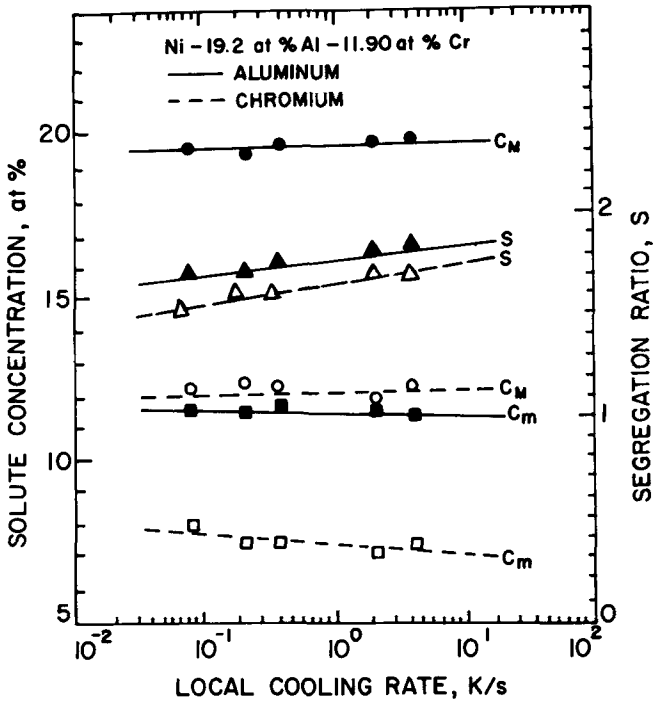

Fig. 9—Aluminum and chromium concentrations C_M and C_m, and segregation ratios S *vs* local cooling rate. Ni-19.2 at. pct Al-11.9 at. pct Cr.

Figure 9 illustrates the dependence of the maximum and minimum solute concentrations, C_M and C_m, respectively, and of the segregation ratio, S, of aluminum and chromium in Ni-19.2 at. pct Al-11.9 at. pct Cr dendritic monocrystals on local cooling rate, $\varepsilon = G \cdot R.$, where G is the average thermal gradient in the solid-liquid zone and R is growth rate. The measurements were conducted at 1661 K in specimens grown at various rates under a thermal gradient of 8×10^3 K/m. It can be seen that C_M remains practically unchanged with increasing ε, C_m slightly decreases,

whereas S slightly increases. The volume fraction nonequilibrium interdendritic γ', g_0, increases with ε (Figure 10). These findings are in agreement with predictions by Brody *et al*[6] whose model assumes back-diffusion of solute during solidification.

C. *Solution Kinetics of the Nonequilibrium Interdendritic γ' Phase*

The solution kinetics of interdendritic nonequilibrium γ' phase were established as described previously.[12] Let g_0 be the volume fraction interdendritic γ' within the cross section corresponding to an isotherm just below the ternary eutectic and g that remaining undissolved at a distance L below this isotherm, hence a time $\theta = L/R$. The fraction residual nonequilibrium interdendritic γ' was plotted *vs* θ in Figure 11 for this monocrystal, as well as those pulled at 0.05 m per hour and 2.00 m per hour. The volume fractions were measured by a systematic point count procedure. Solution kinetics are faster for the rapidly pulled crystal, presumably because primary dendrite arm spacing is then finer and so is the distance over which aluminum has to diffuse during dissolution of γ'.

In order to study isothermally the solution kinetics of interdendritic γ', four monocrystals were pulled at 0.05m per hour under a thermal gradient of 8×10^3 K/m. The first one was quenched; for the other three pulling was arrested for 10 seconds, 20 seconds, and 30 seconds prior to quenching the remaining liquid. The volume fraction interdendritic γ' was measured in transverse cross sections corresponding to 1645 K and 1660 K. Figure 12 illustrates the variation of g/g_0 *vs* time, θ, for these temperatures (curves A and B, respectively), g_0 being the corresponding volume fraction interdendritic γ' for the monocrystal that was continuously pulled and quenched. The same procedure was repeated with monocrystals pulled at 2.00 m per hour, curves C and D. As expected, solution kinetics are faster for higher temperatures and finer dendrite arm spacings.

D. *Homogenization Kinetics*

The diffusion model used herein was described elsewhere.[3] The initial distribution of aluminum and chromium

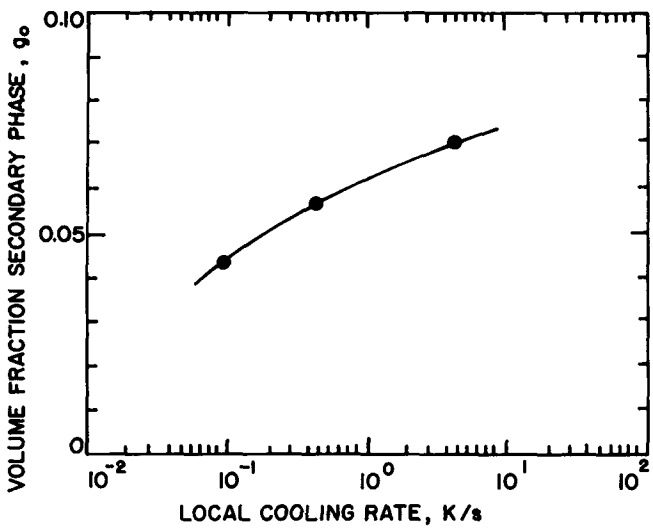

Fig. 10 — Volume fraction of interdendritic nonequilibrium γ' phase, g_0, *vs* local cooling rate. Ni-19.2 at. pct Al-11.90 at. pct Cr.

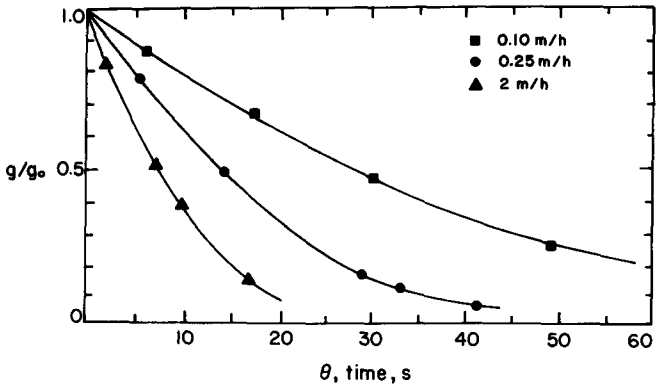

Fig. 11 — Variation of fraction residual nonequilibrium interdendritic γ' *vs* time during crystal pulling. Zero time corresponds to the eutectic isotherm. Pulling rates are: 0.10, 0.25, and 2.00 m/h. Ni-19.2 at. pct Al-11.90 at. pct Cr.

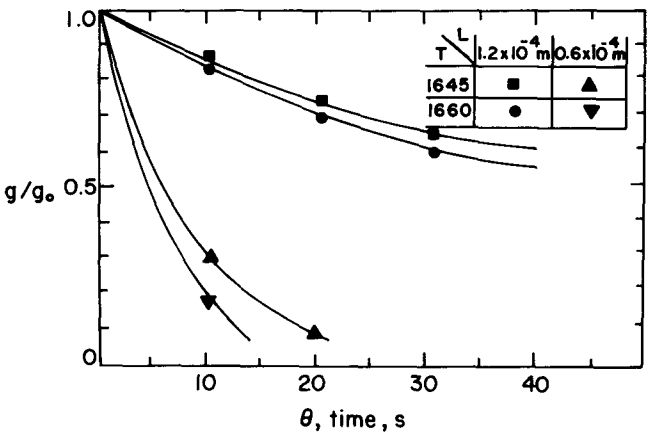

Fig 12 — Variation of fraction residual nonequilibrium interdendritic γ' with isothermal holding time for 2 temperatures. 1645 and 1660 K and 2 microstructures of primary dendrite arm spacings: 2.4×10^{-4}m and 1.2×10^{-4}m. Ni-19.2 at. pct Al-11.9 at. pct Cr.

within the dendritic microstructure of the as-solidified alloy which was used for analytically deriving homogenization kinetics is illustrated in Figure 13. The indices of residual segregation[3] for aluminum and chromium have been calculated in the Appendix and are expressed as follows:

$$\delta_{Al} = 1.04 \exp\left(-\pi^2 \frac{D_{Al}\theta}{L^2}\right) - 0.021 \exp\left(-5\pi^2 \frac{D_{Al}\theta}{L^2}\right) + \ldots$$

$$\delta_{Cr} = 1.037 \exp\left(-\pi^2 \frac{D_{Cr}\theta}{L^2}\right) - 0.037 \exp\left(-5\pi^2 \frac{D_{Cr}\theta}{L^2}\right) + \ldots$$

where D_{Al}, D_{Cr} are the diffusivities of aluminum and chromium at the homogenization temperature, θ is homogenization time, and L is half the primary dendrite arm spacing or half the primary arm spacing, times $1/\sqrt{2}$.[3] Figure 14 illustrates the variation of δ_{Al} and δ_{Cr} *vs* the homogenization parameter θ/L^2 for 1473 K and 1588 K. The experimental

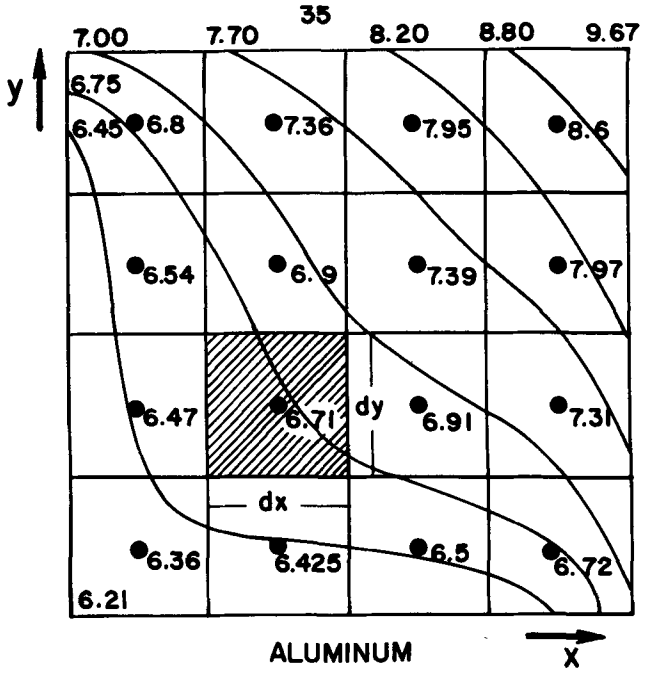

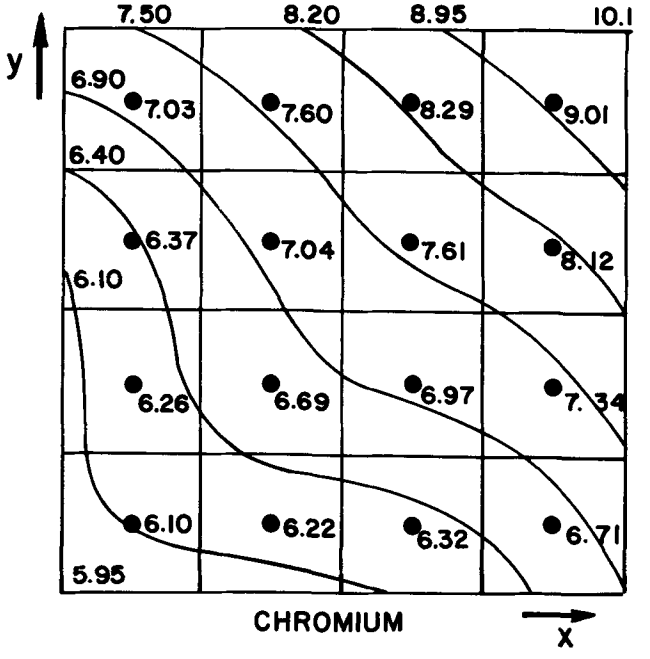

Fig. 13—Isoconcentration curves for aluminum and chromium within a quadrant of the dendritic cross. Ni-14.8 at. pct Al-8.2 at. pct Cr.

points reported on the same graph are for Ni-14.8 at. pct Al-8.2 at. pct Cr dendritic monocrystals exhibiting primary dendrite arm spacings of 240 × 10^{-6}m and 225 × 10^{-6}m. These specimens were homogenized at 1473 K and 1588 K for six and 12 hours. Agreement between experimental points and analytical curves is satisfactory, considering that the adopted diffusion coefficient values may be inaccurate and the geometry of isoconcentration curves depends on growth conditions and location within the dendritic monocrystal.

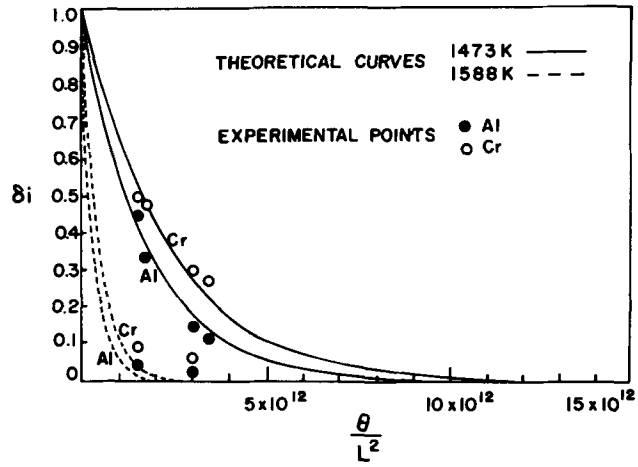

Fig. 14—Index of residual segregation, δ_i, *vs* homogenization parameter, θ/L^2, for aluminum and chromium. Ni-14.8 at. pct Al-8.2 at. pct Cr dendritic monocrystals.

IV. CONCLUSIONS

1. If growth is cellular dendritic, the cellular dendritic spacing exhibits the same dependence on growth rate or local cooling rate as does the secondary dendrite arm spacing in columnar dendrites.
2. An increase in chromium or aluminum concentrations slows down coarsening, yielding finer cast microstructures. At equal atomic percental increase in concentration the effect of chromium is more significant than that of aluminum in refining the dendritic structure.
3. With increasing local cooling rate the maximum solute concentration, C_M, remains practically constant, the mimimum solute concentration, C_M, slightly decreases, the segregation ratio slightly increases, whereas the volume fraction of nonequilibrium interdendritic γ' phase increases substantially.
4. The rate of dissolution of the nonequilibrium interdendritic γ' phase which occurs during crystal pulling increases with increasing pulling or growth rate, due to the finer dendrite spacings.
5. Homogenization kinetics based on a diffusion model which was described previously led to predictions of the index of residual segregation for aluminum and chromium which are fairly close to those measured experimentally on specimens homogenized at 1473 K and 1588 K for six and 12 hours. A longer time is necessary for chromium than for aluminum in order to achieve the same degree of residual segregation.

APPENDIX

Calculation of the index of residual segregation.

A.1 *Aluminum*

The square of corners (0, 0), (L, 0), (L, L), and (0, L) was divided into sixteen partial squares (Figure 13). The solute concentration at any point inside a square was taken as being equal to the concentration at the center of that square. The average concentration of the sixteen squares is $\bar{C}_{Al} = 7.057$ at time 0; the $f_{Al}(x, y) = C^{\circ}_{Al} - \bar{C}_{Al}$ at the different rectangles can then be calculated. Choosing for n and m the

values: 0, 1, 2, the following values of K_{nm} were found: $K_{0,0} = 0$, $K_{0,1} = 0.609$, $K_{0,2} = 0.045$, $K_{1,0} = -0.575$, $K_{1,1} = 0.414$, $K_{1,2} = 0.019$, $K_{2,0} = 0.055$, $K_{2,1} = 0.006$, and $K_{2,2} = -0.016$.

Following the procedure described and applied previously,[3] the index of residual segregation of aluminum is given by:

$$\delta_{Al} = 1.021 \exp\left(-\pi^2 \frac{D_{Al}\theta}{L^2}\right) - 0.021 \exp\left(-5\pi^2 \frac{D_{Al}\theta}{L^2}\right) + \ldots$$

The diffusion coefficient for aluminum adopted here is: $D_L = 1.87 \times 10^{-4} \exp[-32{,}200/T]^7 m^2$ per second. At the homogenization temperatures of 1473 K and 1588 K, $D_{Al} = 5.896 \times 10^{-14}$ m^2 per second and 2.875×10^{-13} m^2 per second, respectively, and:

$$\delta_{Al} = 1.021 \exp[-5.819 \times 10^{-13}(\theta/L^2)] - 0.021 \exp[-29.095 \times 10^{-13}(\theta/L^2)[+ \ldots$$

and

$$\delta_{Al} = 1.021 \exp[-2.8375 \times 10^{-12}(\theta/L^2)] - 0.021 \exp[-14.187 \times 10^{-12}(\theta/L^2)] + \ldots$$

respectively.

A.2 *Chromium*

Following the same procedure as for aluminum, the average concentration of the sixteen squares is $\bar{C}_{Cr} = 7.105$ at time 0; the $f_{Cr}(x, y) = C^\circ_{Cr} - \bar{C}_{Cr}$ at the different rectangles is then calculated. The values found for K_{nm} were: $K_{0,0} = 0$, $K_{0,1} = 0.849$, $K_{0,2} = 0.077$, $K_{1,0} = -0.703$, $K_{1,1} = 0.413$, $K_{1,2} = 0.0302$, $K_{2,0} = 0.017$, $K_{2,1} = 0.026$, and $K_{2,2} = 0.0805$. The following expression was derived for the index of residual segregation of chromium:

$$\delta_{Cr} = 1.037 \exp\left(-\pi^2 \frac{D_{Cr}\theta}{L^2}\right) - 0.037 \exp\left(-5\pi^2 \frac{D_{Cr}\theta}{L^2}\right) + \ldots$$

The diffusion coefficient of chromium adopted here is:[7]

$$6.04 \times 10^{-5} \exp[-30{,}900/T] m^2/s$$

At the homogenization temperatures of 1473 K and 1588 K $D_{Cr} = 4.56 \times 10^{-14}$ m^2 per second and 2.091×10^{-13} m^2 per second, respectively, and:

$$\delta_{Cr} = 1.037 \exp[-4.508 \times 10^{-13}(\theta/L^2)] - 0.037 \exp[-22.542 \times 10^{-13}(\theta/L^2)] + \ldots$$

and

$$\delta_{Cr} = 1.037 \exp[-2.0637 \times 10^{-13}(\theta/L^2)] - 0.037 \exp[-10.318 \times 10^{-12}(\theta/L^2)] + \ldots$$

respectively.

ACKNOWLEDGMENTS

The program on coarsening of dendritic monocrystals was initiated at the Centre des Matériaux, Ecole Nationale Supérieure des Mines de Paris, during a sabbatic leave of one of the authors (TZK). The contribution of M. Jean Massol who processed a series of monocrystals and the assistance of M. G. Lesoult are gratefully acknowledged. The authors are grateful to the Air Force Office of Scientific Research for support through Grant No. 77-3344 to the University of Connecticut where this investigation was conducted.

REFERENCES

1. P. W. Peterson, T. Z. Kattamis, and A. F. Giamei: *Metall. Trans. A*, 1980, vol. 11A, pp. 1059-65.
2. R. Kadalbal, J. J. Montoya-Cruz, and T Z. Kattamis: *Metall. Trans. A*, 1980, vol. 11A, pp. 1547-53.
3. G. D. Merz, T. Z. Kattamis, and A. F. Giamei: *J. Mater. Sci.*, 1979, vol. 14, pp. 663-70.
4. T. Z. Kattamis and J. C. Lecomte: *J Mater. Sci.*, 1978, vol. 13, pp. 2731-36.
5. T. Z. Kattamis, J. M. Coughlin, and M. C. Flemings: *Trans. TMS-AIME*, 1967, vol. 239, pp. 1504-11.
6. H. D. Brody and M. C. Flemings: *Trans. TMS-AIME*, 1966, vol. 236, p. 615.
7. C. J. Smithells: "Metals Reference Book", 5th edition, Butterworths, London, 1976.